Analysis of Hyperion Data with the FLAASH Atmospheric Correction Algorithm

Gerald W. Felde [a], Gail P. Anderson [a], Thomas W. Cooley [b],
Michael W. Matthew [c], Steven M. Adler-Golden [c], Alexander Berk [c], and Jamie Lee [c]

[a] Air Force Research Laboratory, Space Vehicles Directorate, Hanscom AFB, MA 01731
[b] Air Force Research Laboratory, Space Vehicles Directorate, Kirtland AFB, NM 87117
[c] Spectral Sciences, Inc., Burlington, MA 01803

Abstract - A combination of good spatial and spectral resolution make visible to shortwave infrared spectral imaging from aircraft or spacecraft a highly valuable technology for remote sensing of the earth's surface. Many applications require the elimination of atmospheric effects caused by molecular and particulate scattering; a process known as atmospheric correction, compensation, or removal. The Fast Line-of-sight Atmospheric Analysis of Spectral Hypercubes (FLAASH) atmospheric correction code derives its physics-based algorithm from the MODTRAN4 radiative transfer code. A new spectral recalibration algorithm, which has been incorporated into FLAASH, is described. Results from processing Hyperion data with FLAASH are discussed.

I. INTRODUCTION

The Fast Line-of-sight Atmospheric Analysis of Spectral Hypercubes (FLAASH) atmospheric correction algorithm/code is a software package developed by the Air Force Research Laboratory, Space Vehicles Directorate (AFRL/VS), Hanscom AFB and Spectral Sciences, Inc. (SSI) to support the analyses of visible to shortwave infrared (Vis - SWIR) hyperspectral and multispectral imaging sensors [1]. The algorithm derives its first-principles physics-based calculations from the MODTRAN4 [2, 3] radiative transfer code. The main objective of FLAASH is to eliminate atmospheric effects caused by molecular and particulate scattering and absorption from the 'radiance-at-detector' measurements in order to retrieve 'reflectance-at-surface' values.

One of the most important sources of error in atmospheric correction results is uncertainty in the wavelength calibration of the sensor. A typical problem is a constant spectral shift for all channels measured by a given spectrograph. This problem can be caused by a small mechanical misalignment of one or more optical elements in the spectrograph/detector system and can result in wavelength errors of several nm. The effects of wavelength shift errors are generally most severe in regions containing strong atmospheric absorption features. In these regions, spectral artifacts appear upon conversion of the radiance cube to a reflectance cube.

Strong atmospheric molecular absorption features, e.g., the 760 nm oxygen absorption, contain information that can be used to quantify the wavelength error and thus refine the wavelength calibration. By fitting an absorption band shape in the measured radiance spectra to model calculations, the wavelengths can be corrected. This approach was used in the development of a new automated method for hyperspectral wavelength calibration refinement based on in-scene data.

Refining the wavelength calibration by directly modeling the measured radiance would require accurate knowledge of the atmospheric and surface conditions. In order to bypass this requirement, a spectral metric named the Normalized Optical Depth Derivative (NODD) was developed that is insensitive to both the surface reflectance spectrum and the molecular column density. A radiance spectrum is transformed into a NODD spectrum in the following manner:

1. The negative of the natural logarithm is taken. In the limit of a non-scattering atmosphere, this step transforms the spectrum into a superposition of the absorption optical depth and the reflectance spectrum magnitude and shape. The magnitude determines the baseline and, since the reflectance spectrum is typically smooth, the shape mainly affects the slope. In the approximation that the entire molecular absorption band has the same curve of growth (i.e., the square-root law for optically thick pressure-broadened lines), different column densities affect the amplitude of the absorption spectrum but not its shape.
2. Differences between adjacent spectral channels are taken, leading to a derivative-like spectrum. This eliminates the baseline and converts the slope to an offset.
3. The result is mean-subtracted. This eliminates the offset, yielding a spectrum that looks like the derivative of the molecular absorption band and is essentially independent of the surface reflectance.
4. The result is amplitude normalized by scaling to a unit root mean square. In the curve of growth approximation mentioned above, this effectively normalizes to a fixed molecular column density. The resulting spectrum is called NODD.

During testing of the algorithm using AVIRIS data, it was found, as intended, that different pixel spectra and simulations with different water column amounts gave virtually identical NODDs. Sample results for the 1130 nm water band are shown in Fig. 1. The radiance data are taken from 3 different pixels: bare soil, a white painted panel, and a paved road. The absorption features have the same shape in each spectrum but the amplitudes are different because the reflectances are different (ranging from ~0.2 for the road to ~1.0 for the panel). The model simulations are shown for the original wavelength calibration (left) and the best-fit wavelength shift (right). Since the simulations were run for two surface reflectance values (0.5 and 1.0) over a series of water column amounts varying over a factor of 2, there are two families of curves having various absorption depths. It is readily apparent that the best-fit model spectra have the correct absorption band shape, but that a quantitative comparison with the data would be very difficult. The

0-7803-7929-2/03/$17.00 (C) 2003 IEEE

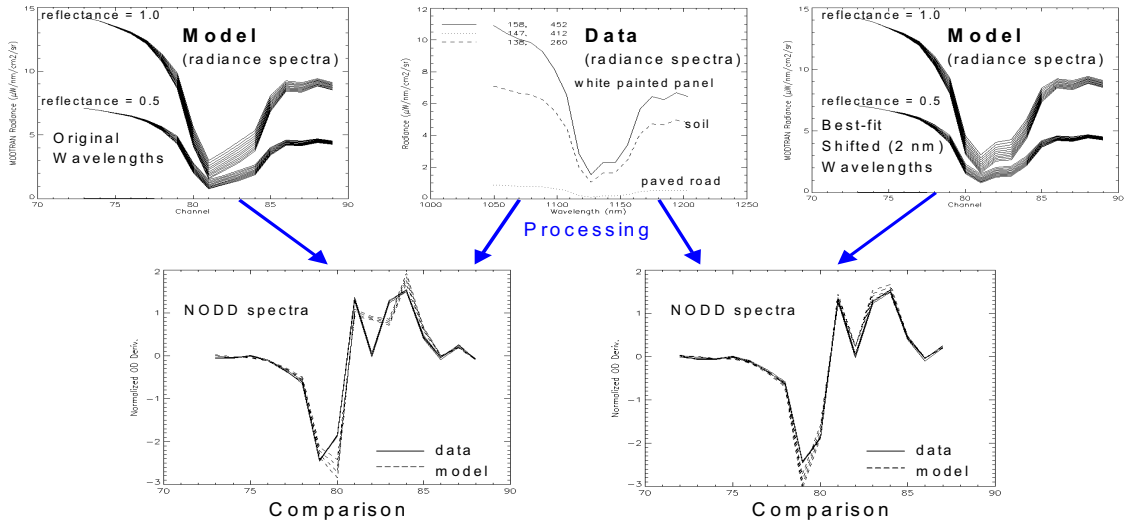

Fig. 1. Sensor wavelength calibration refinement using the 1130 nm water band (example using 3 AVIRIS pixels). The spectra on the left use the original calibration and those on the right use a best-fit wavelength shift of 2 nm. The spectra at the top are in radiance units and those below are in dimensionless units.

NODD spectra shown in the bottom row are much more useful than the radiance spectra shown in the top row. This is because the NODD spectra allow a direct comparison between data and models. All the data NODDs are essentially identical, all the model NODDs for a given wavelength assignment are essentially identical, and the best-fit model NODDs lie virtually on top of the data.

II. FLAASH WAVELENGTH CORRECTION ALGORITHM

An automated wavelength recalibration algorithm based on atmospheric absorption features and the NODD spectral metric has been incorporated into FLAASH. The inputs for this new algorithm are one or more measured radiance spectra, the corresponding MODTRAN4 model calculations, as well as spectrograph information for the sensor and selection of one atmospheric absorption feature for each spectrograph. The wavelength calibration correction algorithm compares measured radiance spectra from one or more pixels in the region of the selected atmospheric absorption band to one or more MODTRAN4 radiance simulations for the same wavelength region using a spectrally flat surface reflectance, approximately correct molecular column densities, and wavelengths shifted by different amounts. However, a direct comparison between the corresponding measured and simulated radiance spectra is not done. Prior to making a comparison, the sets of observed and MODTRAN4 simulated radiance spectra are transformed into NODD spectra. Then for each trial wavelength shift the observed and simulated NODDs are compared. The shift that minimizes the root mean square (RMS) error between them defines the refined wavelength calibration for the sensor.

The output is a single channel offset value, which is expressed as a channel fraction instead of a wavelength, for each spectrometer of the sensor. The wavelength offsets for each spectral channel are calculated by multiplication of the fractional channel offset and the wavelength spacing. Expressing the calibration offset in this manner is prudent if the cause of the offset is misalignment between the optical axis and the focal plane. The difference between a channel fraction and a wavelength is significant for a sensor such as HYDICE whose spectral dispersion varies dramatically within the spectrograph.

The wavelength recalibration option uses a MODTRAN calculation with a surface albedo of 0.15 and the average water vapor from the preliminary retrieval by FLAASH. The preliminary water retrieval is performed with the original wavelength calibration. FLAASH randomly selects ten pixels from a central vertical slice of the image for input to the recalibration algorithm. The wavelength recalibration algorithm is run on the ten pixels, the results are averaged, and a file of a single set of corrected wavelengths for all channels of the sensor is output. The original radiance values and corrected wavelengths are then input into FLAASH to generate the output reflectance cube using the typical cycle of coarse water retrieval, visibility retrieval, and fine water retrieval.

III. FLAASH PROCESSING OF HYPERION DATA

The new wavelength correction algorithm in FLAASH was applied to a Hyperion Level 1B radiance data set, which was collected over the Coleambally, Australia agricultural test site on January 11, 2002 at 23:58 GMT. This data set contains 256 samples x 703 lines x 242 bands. The original Coleambally radiance cube was preprocessed to eliminate bad bands before it was input into FLAASH. VNIR bands 8–56 (427.55 to 915.68 nm) and SWIR bands 78–224 (922.62 to 2395.53 nm) were retained. Also, sample 256 was cut off from every line because they only contain VNIR data. This processing resulted in a subset of the original radiance cube having 255 samples x 703 lines x 196 bands.

Hyperion data contains spectral smile, which is cross-track spatial pixel-dependent wavelength shifts that are a result of curvature or tilt of the entrance slit image on the detector plane. The smile is different for each of the two focal planes. The band wavelength assignments contained in the data set are supposed to be valid for the center pixels (i.e., sample 128). The FLAASH wavelength correction algorithm was applied to the data to quantify the smile and also to check the validity of the wavelength assignments at the center pixels. This was done by dividing the data subset (i.e., 255 samples x 703 lines x 196

bands) into 64 spatial columnar subsets, each four columns wide (minimum image width required by FLAASH is four) and running the wavelength correction algorithm on each of these spatial subsets. The atmospheric absorption features used by the algorithm for the VNIR and SWIR were the 760 nm oxygen region and the 2059 carbon dioxide region, respectively. The resulting wavelength correction values for the VNIR and SWIR are shown in Figs. 2 and 3, respectively.

The VNIR has a pronounced smile. On the other hand, the SWIR has essentially no smile. In fact, the SWIR wavelength corrections are relatively flat over all samples with an approximately constant value of 3 nm. For both the VNIR and SWIR, the original band wavelength assignments contained in the data set are not valid at sample number 128. The VNIR wavelengths are ~2.5 nm too small and the SWIR wavelengths are ~3 nm too small.

Recently, Dr. Robert Green at NASA, JPL (private communication) has determined the Hyperion VNIR and SWIR wavelength calibration errors as a function of spatial pixel number using a different radiance cube. He used a different algorithm but his analysis was also based on a comparison of model and measured radiance spectra in the 760 nm oxygen and the 2100 nm carbon dioxide absorption regions for the VNIR and SWIR, respectively. Green's SWIR results are similar to the results of the current study. His VNIR corrections are also similar to those of the current study, except the magnitude of the corrections are smaller by ~1 nm.

The SWIR wavelength corrections have an approximately constant value of 3.0 nm for all pixel column numbers (Fig. 3). On the other hand, the VNIR wavelength corrections are approximately constant (2.5 nm) only for samples 64 to 128 (Fig. 2). Therefore, the 64 to 128 columnar spatial subset (65 samples x 703 lines x 196 bands) of the Coleambally radiance cube was selected for FLAASH retrieval. A correction of +3.0 nm was applied to the original wavelength assignments of the SWIR channels and a correction of +2.0 nm (average of value found in this study, 2.5 nm, and Green's value, 1.5 nm) was applied to the VNIR channels.

The FLAASH reflectance retrieval was done using the corrected wavelengths and also the original wavelengths along with the adjacency correction option turned on. The reflectance spectra for a soil pixel are plotted in Fig. 4. The results in this figure are without spectral polishing so that the validity of the channel wavelength assignments is readily observable. The spectrum for the original wavelengths contains rapid fluctuations in the strong absorption regions (e.g., 1130 nm water vapor region) but the spectrum for the corrected wavelengths is much smoother in these regions. This indicates that the original spectral calibration is incorrect but that the corrected spectral calibration is good.

IV. CONCLUSION

The new automated spectral recalibration algorithm, which has been incorporated into FLAASH, is an extremely valuable addition. It improves the quality of the output reflectance cube for measured radiance data containing wavelength calibration errors, and it also can be used as a tool to measure varying wavelength shifts in the cross-track spatial dimension of an image, such are found in data from the Hyperion sensor and others that use 2-dimensional detector arrays.

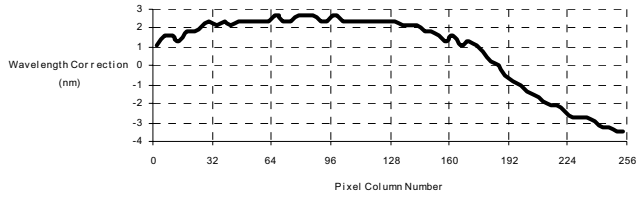

Fig. 2. Hyperion VNIR wavelength corrections (based on 760 nm oxygen absorption feature).

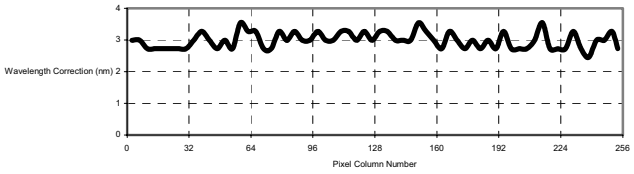

Fig. 3. Hyperion SWIR wavelength corrections (based on 2059 nm carbon dioxide absorption feature).

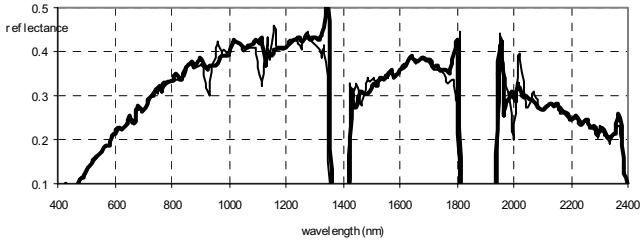

Fig. 4. Reflectance spectra for corrected (thick line) and original (thin line) wavelength assignments for a soil pixel.

ACKNOWLEDGMENT

The work at Spectral Sciences, Inc. was supported by the U.S. Air Force Research Laboratory under contracts F19628-99-C-0031 and F19628-00-C-022.

REFERENCES

[1] M.W. Matthew, M. S. M. Adler-Golden, A. Berk, S. C. Richtsmeier, R.Y. Levine, L. S. Bernstein, P. K. Acharya, G. P. Anderson, G. W. Felde, M. L. Hoke, A. J. Ratkowski, H.-H. Burke, D. Miller J. H. Chetwynd, Status of Atmospheric Correction Using a MODTRAN4-based Algorithm, In Algorithms for *Multispectral, Hyperspectral, and Ultraspectral Imagery VI*, Sylvia S. Chen, Michael R. Descour, Editors, Proceedings of SPIE Vol. 4049, pg. 207, 2000.

[2] A. Berk, L.S. Bernstein, D.C. Robertson, P.K. Acharya, G.P. Anderson, and J.H. Chetwynd, "MODTRAN Cloud and Multiple Scattering Upgrades with Application to AVIRIS," Summaries of the Sixth Annual JPL Airborne Earth Science Workshop, JPL Publication 96-4, Vol. 1, Pasadena, California, pp. 1-7, 1996.

[3] G.P. Anderson, A. Berk, P. K. Acharya, M. W. Matthew, L. S. Bernstein, J. H. Chetwynd, H. Dothe, S. M. Adler-Golden, A. J. Ratkowski, G. W. Felde, J. A. Gardner, M. L. Hoke, S. C. Richtsmeier, B. Pukall, J. Mello and L. S. Jeong, MODTRAN4: Radiative Transfer Modeling for Remote Sensing, In Algorithms for *Multispectral, Hyperspectral, and Ultraspectral Imagery VI*, Sylvia S. Chen, Michael R. Descour, Editors, Proceedings of SPIE Vol. 4049, pg. 176-183, 2000.